New Journal of Glass and Ceramics, **2011, 1, 69-78**
doi:10.4236/njgc.2011.12012 Published Online July 2011 (http://www.SciRP.org/journal/njgc)

Physical Study of Thin Film and Monolithic Nano-Composites [SiO_2:11P_2O_5:3Al_2O_3:(1.2)Er (1.2, 1.8 and 3)Yb] Prepared by Sol Gel Technique, Planar Waveguide and Co-operative Up-Conversion

Y. Badr[1], I. K. Battisha[2], A. M. S. El Nahrawy[2], M. Kamal[3]

[1]National Institute of Laser Enhancement Sciences (NILES), Cairo University, Cairo, Egypt; [2]National Research Center (NRC) Department of Solid State Physics, Doki, Giza, Egypt; [3]Physics Department El Manssoura University, Egypt.
Email: szbasha@yahoo.com

Received May 21st, 2011; Revised June 18th, 2011; Accepted June 25th, 2011.

ABSTRACT

Nano-composite silica-phosphate system (SiO_2-P_2O_5) *co-doped with* Al_2O_3 *as a host material and prepared by sol gel technique in two forms monolith and thin film using multilayer spin-coating method were activated by* Er^{3+} *and* Yb^{3+} *ions as in the formula*; [SiO_2:11P_2O_5:3Al_2O_3:(1.2)*Er*:(1.2, 1.8 *and* 3)*Yb*]. *The prepared samples have been synthesized using tetra-ethyl-orthosilicate* (*TEOS*) *and triethyl-phosphate* (*TEP*) *as precursor sources of silica and phosphorus oxides. The microstructure and crystallinity of the prepared samples will be characterized by using x-ray diffraction* (*XRD*) *which, imply that the crystallite sizes of* [SiO_2:11P_2O_5:3Al_2O_3:(1.2)*Er*:(1.2)*Yb*] *at* 500℃ *for both thin film and monolith forms of the prepared samples were found to be equal to* 35 *and* 33 *nm, respectively. The refractive index will be evaluated by measuring the normal transmission and specular reflection of the prepared samples. The photoluminescence properties have analyzed in the visible wavelength range between* 500 *and* 800 *nm as a function of sample composition.*

Keywords*: *Sol-Gel*, *Silica-Phosphate*, *Rare Earth*, *XRD*, *Photoluminescence*, *Waveguide*, *Co-Operative Up-Conversion

1. Introduction

In the last decade, various technologies have been employed for the fabrication of silica (SiO_2) based integrated optics (IO) components and a broad variety of silicate glass systems have been investigated. So silica-phosphate glasses doped with rare earth have been favored in the development of integrated waveguide amplifiers, where the rare-earth concentration must be orders of magnitude higher than in fibers [1]. Glasses synthesized by the sol–gel method are promising matrices for the formation of optical nano-composites. The use of these nano-composites in optoelectronics, photonics and fiber optics has opened up the new way for the development of unique information systems with tunable characteristics over a wide frequency range [2]. Sol-gel processing, has been shown to be a relatively inexpensive method to prepare such IO components [3,4], which may allow the incorporation of RE ion concentrations higher than those possible by conventional glass melting methods, but at the same time the stronger ion-ion interactions may reduce the RE fluorescence performance, by decreasing its intensity and lifetime. Photonic materials for optical amplifiers' based on rare-earth (RE) ions such as Er^{3+}, are in wide use today, especially for dense wavelength division multiplexing (DWDM) applications. However, the small absorption cross sections of Er^{3+} ions have become a limitation to the optimization of such materials for optical amplification and, therefore, a number of methods have been proposed to increase the excitation efficiency of Er^{3+} ions [5]. It was previously reported that, the wavelength of the main Er^{3+} ground-state transition, 1.54 μm, coincides with the standard wave-

length use in optical telecommunication systems determined by the quartz waveguide transparency window. The Er^{3+} ion can also efficiently emit light at other discrete wavelengths in the visible and near-IR spectral regions determined by the structure of the excited states of this ion as in our case in the present work [6]. Erbium-ytterbium (Er^{3+}:Yb^{3+}) doped fiber lasers and amplifiers show a growing potential for many applications in different areas such as industry, light emitting devices, communication, military and research [7-9]. In order to improve the luminescence performance of Er^{3+} ions doped sol-gel silica-phosphate planar waveguides, co-doping achieved with Al [10,11]. However, it would be difficult to enhance the emission efficiency of Er^{3+} ions due to its low absorption cross-section. A good alternative method to overcome this problem is to co-dope Yb^{3+} with Er^{3+} into a material. The ytterbium ion has a strong absorption so it can use as a sensitizer for other luminescent ions. Co-doping with Yb^{3+} has been shown to increase the photoluminescence (PL) emitted by the rare earth like Er^{3+} ions [12].

In the present work a preliminary study of silica-phosphate co-doped with Al^{3+} ions as a host material, activated by doping it with constant concentration of Er^{3+} ions at 1.2 mol% and different concentrations of Yb^{3+} ions at (1.2, 1.8 and 3) mol%, respectively and prepared by sol-gel technique in two different forms thin film and monolith. The results investigated using XRD, in order to assess the structural properties. The photoluminescence of the prepared samples in the visible and infrared wavelengths ranges will compared and evaluated. The co-operative up-conversion emission spectra exhibited the green emission bands assigned to $^2H_{11/2}\rightarrow{}^4I_{15/2}$ and $^4S_{3/2}\rightarrow{}^4I_{15/2}$ transitions and group red emission bands between 600 nm and 800 nm that were attributed to the $^4F_{9/2}\rightarrow{}^4I_{15/2}$ transitions of Er^{3+} ions, respectively was detected. All obtained data will be analyzed and compared.

2. Experimental

Silica-phosphate (SiO_2: $11P_2O_5$) doped with 3 mol% Al^{3+} ions, as a host materials was prepared by sol-gel technique in two different forms monolithic and thin film, it is activated by constant concentration 1.2 mol% of Er^{3+} ions using the synthesizer Yb^{3+} ions at different concentrations (1.2, 1.8 & 3 mol%) planar wave guide. The prepared samples were obtained by hydrolysis and poly-condensation of tetraethoxysilane (CH_3CH_2OH)4Si (TEOS, 99.999%, Sigma-Aldrich) as SiO_2 precursor and Triethyl-phosphate $(C_2H_5O)_3P(O)$ as P_2O_5 precursor in ethanol. The solution were hydrolyzed under vigorous stirring with distilled H_2O containing HCl, which is used as a catalyst as described in **Figure 1**. In the case of doping with the Er^{3+} and Yb^{3+} ions all preceding experimental steps as-synthesized sol was then doped with 3 mol% $Al(NO_3)_3$-H_2O, to aid in eliminating the presence of hy droxyl groups and also favor the dispersion of doping ions in the matrix. Then the Er^{3+} and Yb^{3+} ions were introduced in the process, by dissolving Er $(NO_3)_3$-H_2O and $Yb(NO_3)_3$-H_2O solutions in to the preceding mixture precursors with molar ratios 1.2 mol% Er^{3+} and (1.2, 1.8 and 3 mol%) Yb^{3+}, respectively. These solutions then filtered, followed by stirring for one hour at room temperature RT. The resultant homogeneous solutions of monolithic materials filled in molds and aged in RT for one week before dried in the oven type GFL 71.5, at about 60℃ for 21 days until no shrinkage appears. The final products were monolithic samples. Samples were clear, transparent, with faint rose color and without cracks. Densification of gel obtained by annealing in air for 3 h at temperature ranging from 100˚C up to 900˚C in a muffle furnace with heating rate 1.5℃/min. Preliminary crystallization obtained by heating the samples at 300℃ for 3 hours. In case of the thin film optical treated silica substrates and glass substrates were used as substrates for the deposition of silica-phosphate doped with (Er^{3+}:Yb^{3+}) solution, using the same solution as for the preparation of monolithic. This solution dispersed on the substrate and then spun at 3500 rev./min for 30 seconds in a clean room by using the spin coating. At least two successive coatings were required to provide suitable effective film thickness. After finishing the coating procedure, the substrates dried for 30 min at 600℃ and then heat-treated at different heat treatment temperature from 100℃ up to 5000℃, giving crack free, homogeneous and transparent enough for waveguide thin films, respectively.

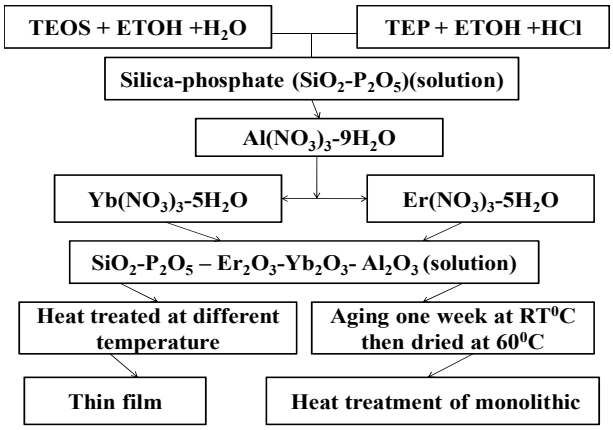

Figure 1. Flow chart for the preparation of monolithic and thin film [SiO_2: $11P_2O_5$: $3Al_2O_3$: (1.2) Er (1.2, 1.8 and 3) Yb], using sol gel method.

X-ray diffraction (XRD) patterns from the prepared samples were recorded with Philips X-ray diffractometer PW/1710; with Ni filter, with monochromatised CuKα radiation of wavelength 1.54045 Å at 40 KV and 30 mA. Crystallite sizes *G* were determined from the Scherrer's equation

$$(G = K\lambda/D\cos\theta),$$

where λ is the wavelength, and *D* is the (corrected) full width (in radians) of the peak at half maximum (FWHM) intensity. The correction to the measured FWHM *Ds* for a sample peak was made to accommodate systematic instrumental broadening and utilized peak widths *Dq* measured from a diffraction scan, taken under identical conditions, from a strain-free powdered quartz sample, with crystallite size ranging between 5 and 10 lm. The corrected sample peak widths were calculated as

$$(D = D_s^2 - D_k^2)^{1/2}$$

Micro-strain and crystallite size contributions to *D* separated using the Win-Fit program, using standard samples for estimation of instrumental broadening. The final sample crystallite sizes *G* obtained by Fourier analysis, using the corrected profile. Nearly normal transmittance and reflectance spectra were done by Jasco V-570 spectrophotometer, in wavelength range (0.2 - 2.5 μm). The transmission electron microscope (TEM) allows the user to determine the internal structure of materials. TEM was performed by using a JEOL JEM-1230 operating at 120 KV attached to CCD camera.

For photoluminescence (PL) measurement, the sample excited by the 488 nm line of a Spectra Physics 2017 Argon laser used to excite room temperature luminescence spectra. A fiber optic probe coupled to a Dilor Superhead, equipped with a suitable notch filter, employed. The scattered signal analyzed by a Jobin-Yvon HR 460 mono-chromator and a spectrum one CCD detector. A 150 line/mm grating used to collect the laser-excited luminescence spectra, whilst for high-resolution luminescence spectra a 1200 lines/mm grating employed. The PL emission obtained using lock-in amplifier (SR 510-Stanford) technique and recorded by computer. The measurements performed at room temperature.

3. Results and Discussion

3.1. XRD Results

Figures 2 and **3** show the XRD patterns of monolithic(SiO_2:11P_2O_5:3Al_2O_3:1.2Er_2O_3) doped with different concentrations of Yb^{3+} ions as in the formula(SiO_2: 11P_2O_5:3Al_2O_3:(1.2)Er(1.2, 1.8 and 3)Yb), sintered at different heat treatment temperatures (100˚C, 300˚C and

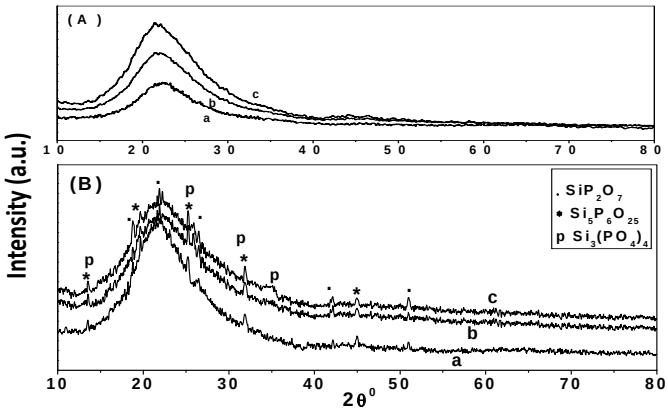

Figure 2 (A, B). XRD patterns of monolithic SiO_2:11P_2O_5:3Al_2O_3 doped with (a) 1.2Er^{3+}:1.2Yb^{3+} (b) 1.2Er^{3+}:1.8$Yb^{3+}$and (c) 1.2Er^{3+}:3Yb^{3+}, sintered at (A) 100˚C and (B) 300˚C for 3 h; p $Si_3(PO_4)_4$ phase, * $Si_5P_6O_{25}$ phase and • SiP_2O_7 phase.

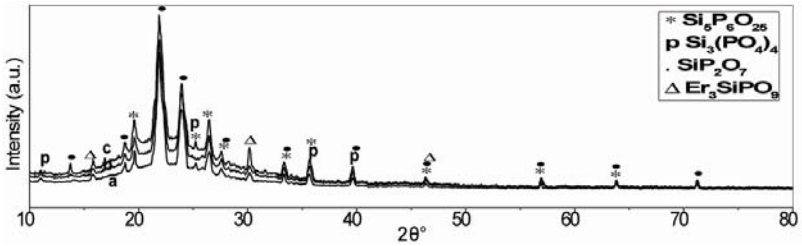

Figure 3 (a, b and c). XRD patterns of monolithic SiO_2:11P_2O_5:3Al_2O_3 doped with (a) 1.2 Er^{3+}:1.2Yb^{3+} (b) 1.2Er^{3+}:1.8Yb^{3+} and (c) 1.2Er^{3+}: 3Yb^{3+}, sintered at 700˚C for 3 h; p $Si_3(PO_4)_4$ phase, * $Si_5P_6O_{25}$ phase, Δ Er_3SiPO_9 phase and • SiP_2O_7phase.

700˚C) for 3 h. When silica-phosphate doped with (Er^{3+}:Yb^{3+}) ions subjected to heat treatment for densification, many properties of the gel changed as a result of structural changes in the host skeleton of a gel which, is attributed to the development of cross-linking of the Si-O and P-O bonds due to dehydration poly- condensation of the system. The curves sintered at 100˚C show broad hump at 2θ between 18˚ and 30˚ attributed to amorphous matrix. By increasing the temperature up to 300˚C very weak peaks of silica-phosphate begin to appear due to the presence of silica-phosphate nanocompounds. Assigned to (hexagonal silica phosphate) $Si_3(PO_4)_4$ and (rhombohedra silica phosphate) $Si_5P_6O_{25}$ phases according to JCPDS cards- number (22 - 1380) and (70 - 2071). These phases consists of isolated SiO_6 and Si_2O_7 units linked by PO_4 groups in the system silica-phosphate [13-15] to form SiO_2-P_2O_5 nano- composite [16,17] in addition of the presence of monoclinic silica phosphate (SiP_2O_7) phase according to JCPDS card number (71 - 2073). Above 300˚C, the crystallization in silica-phosphate gel glasses greatly changed the coordination of Er^{3+}:Yb^{3+} ions. An Er^{3+}:Yb^{3+} ions situated in a binary system composed of crystalline and glass phase. Another effect of increasing the temperature of the samples is that the intensity of the XRD peaks increased due to the continually change in the chemical structure and the rearrangements of the crystalline system. Then the prepared samples become crystalline, with separation of the phases; according to the diffraction peaks as shown in **Figure 3**. By increasing the sintering temperature up to 700˚C, the intensity of XRD patterns increase giving rise to crystallinity enhancement. Separation of the phases; according to the diffraction peaks, the (hexagonal silica-phosphate) $Si_3(PO_4)_4$ phase was eliminated by increasing the temperature and the (rhombohedra silica phosphate) $Si_5P_6O_{25}$, (silica phosphate) SiP_2O_7 phases increase and a new phase (monoclinic erbium silica phosphate) Er_3SiPO_9 appeared due to the effect of the Er^{3+} ions, according to JCPDS cards no.(49 - 0206).

Figures 4 and 5 show the XRD patterns for some thin films silica-phosphate system co-doped 3 mol% Al_2O_3 with 1.2 mol% Er^{3+}:(1.2 & 1.8)Yb^{3+} ions samples as in the following formula; (SiO_2:11P_2O_5:3Al_2O_3:1.2Er_2O_3:(1.2 & 1.8)Yb_2O_3) prepared from the same precursors, sintered at different heat treatment temperatures, 100˚C, 150˚C, and 500˚C for 3 h. The behavior of the prepared thin film samples after dried at low sintered temperature 100˚C and 150˚C, give nearly the same trend of the monolithic samples observed where the samples were still in the amorphous state and have larger specific area. By increasing the sintered heat treatment temperature up to 500˚C, the intensities of the $Si_3(PO_4)_4$, $Si_5P_6O_{25}$ and SiP_2O_7 phases increase with increasing the sintering heat treatment temperature. While, the initial state of a film generally denser and less cross-linked than a bulk gel made from the same sol, and this transport path of heat through the thickness of the film. Where, these films have been prepared from the same precursor of preparing the monolith samples by aging two days after spinning. The observed change in the XRD peaks height as well as the broadening could interpreted by the adsorption of the incorporated atoms on the surface of the growing silica-phosphate doped with REEs gel microcrystal. The thinner of the film thickness may be preventing it to grow larger along or perpendicular to the substrate compared with the monolithic form samples. We found that the crystallizations growth in the thin film was faster and more intense due to the thinner thin film than the monolithic, where the film is denser and has smaller pores, Figure of XRD of monolith sample sintered at heat treatment temperature 500˚C not shown here due to the large number of figures presented.

By confirming the crystallite size data calculated by Scherrer's equation ($G = K\lambda/D\cos\theta$), and by using the Win-fit programmer for [SiO_2:11P_2O_5:3Al_2O_3:(1.2)Er (1.2)Yb] at constant sintering temperature 500˚C for both thin film and monolith the crystallite sizes were found to be equal to 35 and 33 nm, respectively [18-21].

3.2. Optical Properties

Figure 6(A) and **(B)** show the optical transmission and reflection spectra of the investigated (A) [SiO_2:11P_2O_5:3Al_2O_3:(1.2)Er(1.2, 1.8 and 3)Yb] and (B) [SiO_2:11P_2O_5:3Al_2O_3:(1.2)Er(1.8)Yb] thin film sintered at 100˚C for the former and at different heat treatment temperature 300˚C and 700˚C for the later. The film deposited on glass and optical treated silica substrates. The transmittance data corrected relative to the optically identical uncoated substrate. It was observed that the transmission showed lower interference fringes that are disturbed by the absorption of OH in silica-phosphate doped with (Er^{3+}:Yb^{3+}) ions while higher transmittance was obtained at lower temperature. The OH eliminated by increasing the sintered heat treatment temperature. This indicates that the optical path of silica-phosphate glass and doped with some Er^{3+} and Yb^{3+} ions increases by increasing temperature. Furthermore, the transmitted intensity decreases with increasing temperature, mainly due to the light scattering increased in silica-phosphate doped samples and might be due to the poly-condensation and densification produced by increasing the sintered temperature, resulting in changing the faint rose color tobe dark rose as discussed in the experimental part Section 2. This result is in agreement with XRD results ob-

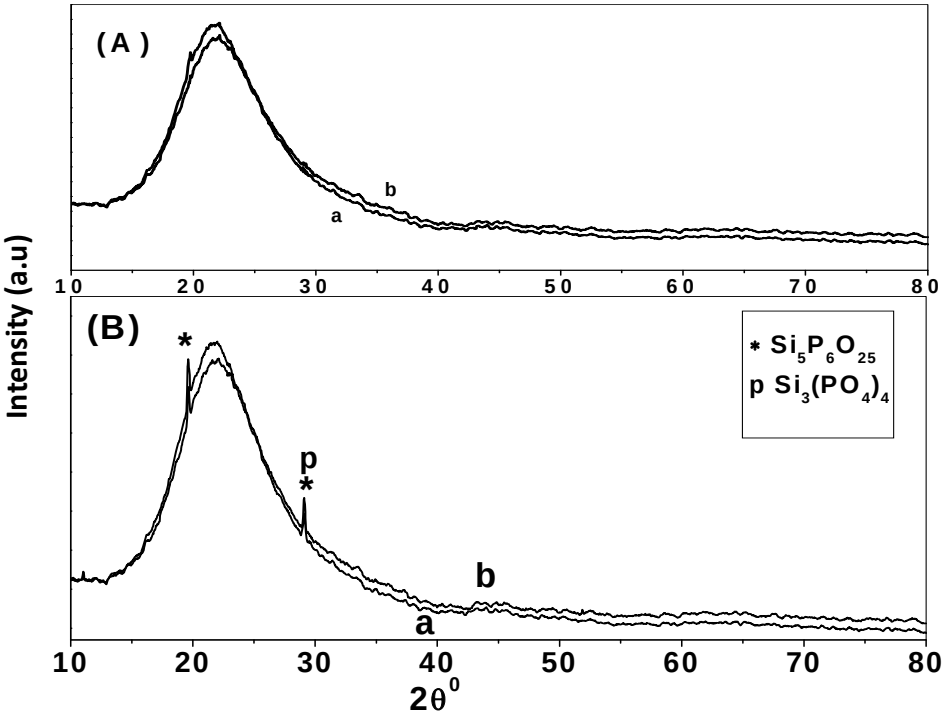

Figure 4 (A, B). XRD patterns of thin film SiO_2:$11P_2O_5$:$3Al_2O_3$ doped with (a) $1.2Er^{3+}$:$1.2Yb^{3+}$ and (b) $1.2Er^{3+}$:$1.8Yb^{3+}$, sintered at (A) 100˚C and (B) 150˚C for 3h; p $Si_3(PO_4)_4$ phase, * $Si_5P_6O_{25}$ phase.

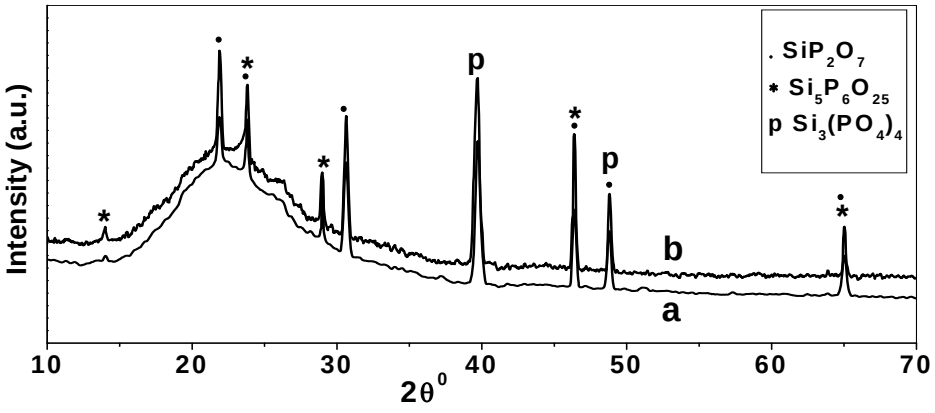

Figure 5. XRD patterns of thin film SiO_2: $11P_2O_5$:$3Al_2O_3$ doped with (a) $1.2Er^{3+}$: $1.2Yb^{3+}$ and (b) $1.2Er^{3+}$: $1.8Yb^{3+}$, sintered at 500˚C for 3 h; p $Si_3(PO_4)_4$ phase, * $Si_5P_6O_{25}$ phase, • SiP_2O_7 phase.

tained in the present work.

The behavior of the refractive index (n) for (SiO_2: $11P_2O_5$:$3Al_2O_3$:(1.2)Er:(1.2, 1.8 and 3)Yb), sintered at different temperature ranging from 100˚C up to 700˚C was shown in **Figure 7**. By increasing the sintering temperature and the concentration of the synthesizer Yb^{3+} ions the refractive index increases due to the increase in the crystallization degree. The sample presents a good variation of the refractive index illus trating the preparation of a single mode silica-phosphateglasses doped with Er^{3+}:Yb^{3+} ions planar waveguide. The refractive index linearly increased with increasing densification, condensation, temperature and increasing the Yb^{3+} ions concentrations indicated the change in chemical structure and the rearrangement of the host sample when incorporated with different Er^{3+}:

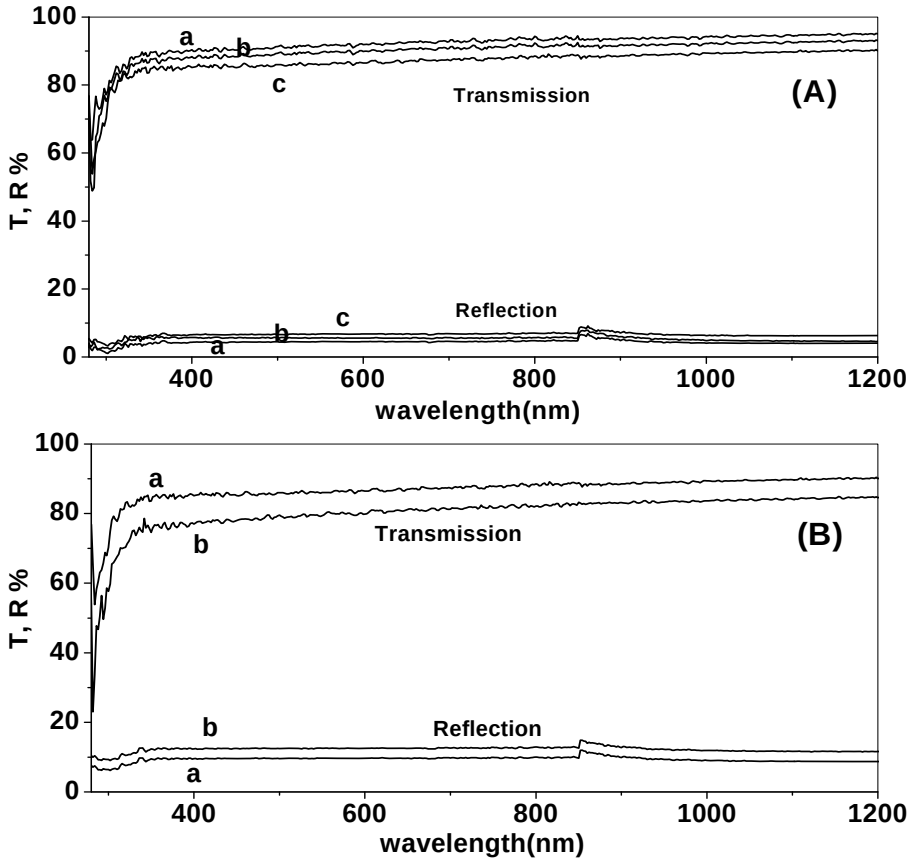

Figure 6 (A, B). Optical transmission & reflection spectra for (A) [SiO_2:11P_2O_5:3Al_2O_3:(1.2)Er: ((a) 1.2), (b) 1.8 and (c) 3 Yb], all sintered at 100˚C and (B) [SiO_2:11P_2O_5:3Al_2O_3:(1.2) Er:(1.8)Yb], sintered at heat temperature (A) 300˚C and (B) 700˚C.

Yb^{3+} ions concentration [22,23]. This creates a more rigid network and causes a decrease in the molar volume, leading to higher refractive index [24].The values of refractive index (n) of thin film samples are given at wavelength = 500 nm. It was found that it increases by increasing the sintered temperature and the Yb^{3+}ions concentration ranging between the following values 1.55 up to 1.68 for silica-phosphate doped with Er^{3+}:Yb^{3+} ions and increasing temperature as shown in **Table 1** and **Figure 7**. This increase is associated with the condensation and densification of the materials, which enhanced by doping the silica-phosphate with different REEs ions and increasing temperature. The obtained data allow the preparation of low loss coupling systems planar waveguide [25]. The refractive index (n) at wavelength = 500 nm of [SiO_2:11P_2O_5] thin film and monolith samples sintered at 500˚C were equal to 1.65 and 1.59, respectively.

3.3. Photoluminescence Spectra

Figures 8 and **9** show the photoluminescence (PL) emission spectra of monolithic and thin film samples as in the following formula [SiO_2:11P_2O_5:3Al_2O_3:(1.2)Er: (a) 1.2Yb and (b) 3Yb], both sintered at temperature 200˚C. It is well known that the absorption cross-section of Er^{3+} ions is small, for that Yb^{3+} ions was used as a sensitizer to increase the Er^{3+} ions PL emission under Argon laser excitation at wavelength (488 nm) [12,26]. It has been well addressed that the green emissions at 542, 552 and 571 nm have been attributed to the intra-4F-transitions

Table 1. The values of refractive index for thin film [SiO_2: 11P_2O_5:3Al_2O_3:(1.2)Er:(1.2, 1.8 and 3Yb], sintered at different temperature.

Samples	(SiO_2:11P_2O_5:1.2Er_2O_3:(1.2, 1.8 & 3)Yb_2O_3:3Al_2O_3)		
T˚C	1.2Er^{3+}:1.2Yb^{3+}	1.2Er^{3+}: 1.8Yb^{3+}	1.2Er^{3+}: 3Yb^{3+}
100	1.55	1.57	1.59
200	1.56	1.59	1.61
300	1.58	1.61	1.63
500	1.61	1.63	1.65
700	1.64	1.66	1.68

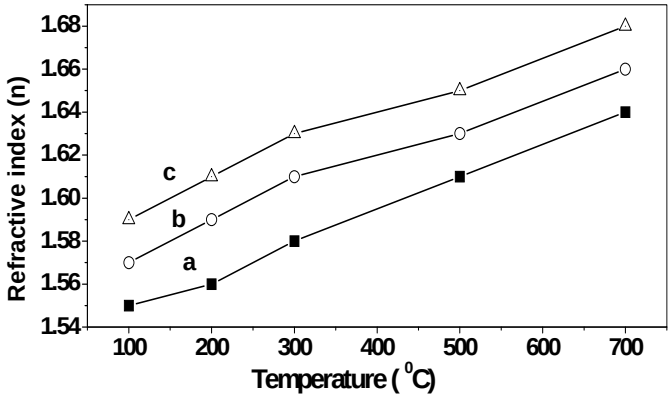

Figure 7. The refractive index as a function with temperature for thin film (SiO_2:11P_2O_5:3Al_2O_3:1.2Er) doped with different concentrations of Yb ions (a) 1.2 (b) 1.8 and (c) 3 mol%, sintered at different temperature.

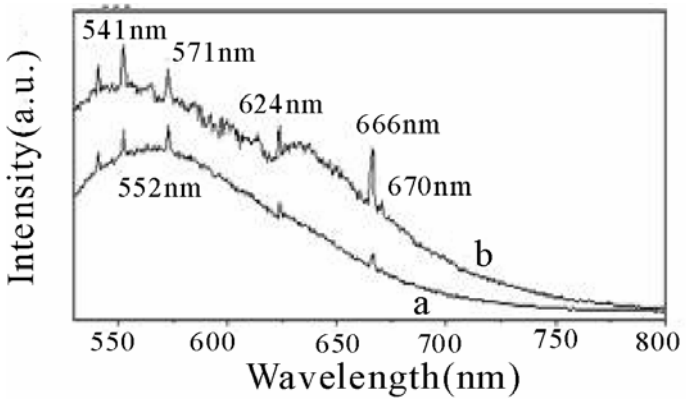

Figure 8. The room-temperature visible and NIR emission spectra of the monolith [SiO_2:11P_2O_5:3Al_2O_3:(1.2)Er:((a) 1.2 and (b) 1.8)Yb], sintering at temperatures 200˚C.

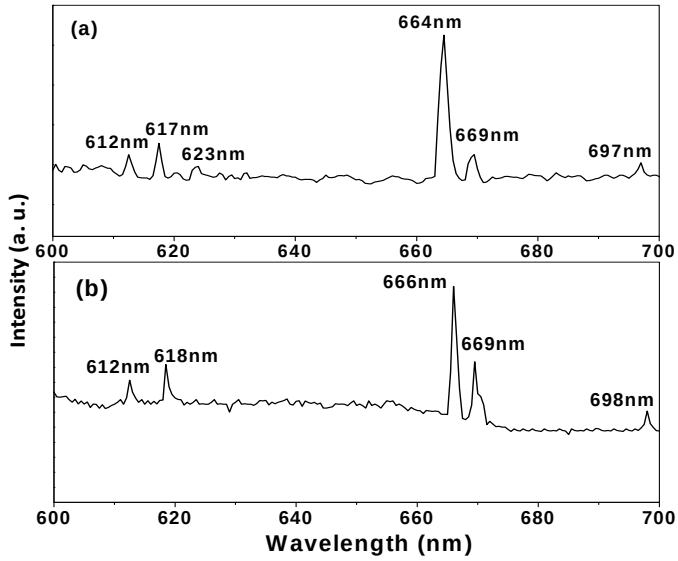

Figure 9. Room-temperature PL emission spectrum of thin film (SiO_2:11P_2O_5:3Al_2O_3:1.2Er_2O_3) doped with two different concentrations of Yb_2O_3 (a) 1.2 (b) 1.8 mol%, sintered at temperature, 200˚C.

of Er^{3+} ions and were assigned to the ($^4S_{3/2}\rightarrow{}^4I_{15/2}$) (542 and 571 nm) and ($^2H_{11/2}\rightarrow{}^4I_{15/2}$) (542 nm) respectively for monolithic sample. The group red emission is attributed to a transition of Er^{3+} ions assigned to ($^4F_{9/2}\rightarrow{}^4I_{15/2}$) in region between 600 and 800 nm with higher intensity in both form of samples thin film and monolith at (666 nm), which is dominant in all spectra [27]. In low sintering temperature the Er^{3+} ions doping has multiplicity of the sites and environments due to the disordered nature of Er^{3+} ions located in the multi-phases. To compare between the green and red PL emission we can propose two mechanisms; first one, for dominant green luminescence in which, the laser light brings the Er^{3+} ion in to $^4I_{9/2}$ level, which then decays through a non-radiative process into the $^4I_{11/2}$ metastable levels and subsequently into the $^4I_{13/2}$ metastable level. Energy transfer processes bring the Er^{3+} ion into ($^4F_{7/2}$) state from which ($^4S_{3/2}$) is populated through the non-radiative relaxation. The second mechanism for the dominant red luminescence one is that the laser beam brings the Er^{3+} ion to the excited state $^4I_{9/2}$ level. One ion non-radiatively decays to the $^4I_{11/2}$ metastable level, and the second decays to the $^4I_{13/2}$ metastable levels. Energy transfer processes bring the Er^{3+} ion to the $^4F_{9/2}$ and a red emission can observed. The spin-allowed radiative transition from the preceding levels to the ground state gives rise to the visible and red PL emissions, respectively. The energy transfer (ET) between two close ions also takes place and plays a significant role in the PL emission. It was observed that the $^4F_{9/2}$ is predominantly excited in this material with the high intensity of the $^4F_{9/2} \rightarrow {}^4I_{15}$ transition. The absorption 488 nm radiation results in the $^4I_{11/2}$ (Er) level, with population proportional to the pump power. The de-excitation of the $^4I_{11/2}$ (Er) level, via no-radiation multi-phonon relaxation, takes the population of the $^4I_{13/2}$ (Er) level. The absorption of the second photon (~ 488 nm) promotes the excitation in the $^4F_{9/2}$ (Er) level, resulting in the group red emission with its maximum at (~ 666 nm) [28]. The ESA approach occurs only during excitation, whereas the ET can happen both during and after excitation.

The red emission is much stronger than green emissions, which may be due to effect of doping the prepared samples with Yb^{3+} ions and the intense of the spectra increased with increasing the Yb^{3+} concentrations. The introduction of Yb^{3+} in silica-phosphate host brings great changes for the photoluminescence properties of Er^{3+} ions and a moderate green to red light can be seen in monolithic sample under the same excitation. Where the multiplicity of RE sites in the host matrix are known to enhance the inhomogeneous broadening of the emission and absorption lines [29,30] and a red shift was observed for the emission lines. Once Er^{3+} and Yb^{3+} ions were excited, they relaxed to ground state, emitting the infrared emissions. The emission of ytterbium was cross-relaxed and the electrons in the $^4I_{11/2}$ level of erbium increased their energy to the $^2F_{7/2}$ level [31]. In order to improve the photoluminescence performance of Er^{3+} doped sol-gel silicate planar waveguides, co-doping achieved with Yb and Al or P [29,31]. The RE ion Yb^{3+} is known to have a significant sensitizing effect on Er^{3+} ions doped glasses [12,32], are attributed to the intra f-f transitions of Er^{3+} And Yb^{3+} ions. Some of emissions bands in visible region were disappeared in thin film sample, due to easy elimination of OH^- groups and the densification resulting in the rearrangement of the structure.

3.4. Co-Operative Up-Conversion Emission of Monolithic [SiO2:11P2O5:3Al2O3:1.2 Er:1.8Yb]

The effect of another existing source on the monolithic (SiO_2:11P_2O_5:3Al_2O_3:1.2Er:1.8Yb) sample using the laser diodes with excitation at 808 nm presented as follow in **Figure**. **10**, which shows the room temperature co-operative up-conversion spectra of the monolithic [SiO_2:11P_2O_5:3Al_2O_3:1.2Er:1.8Yb], sintered at temperature 300˚C. The green emission in the range between 550 and 570 nm attributed to the $^4S_{3/2}\rightarrow{}^4I_{15/2}$ transition. The visible up-conversion emission band at 589 nm is the maximum one, which can attributed to the $^4S_{3/2}\rightarrow{}^4I_{15/2}$ transition of Er^{3+} ions and a group red emission in the region between 600 - 650 nm assigned to another intra-4f transition $^4F_{9/2}\rightarrow{}^4I_{15/2}$.

The up-conversion emission of Er^{3+} and Yb^{3+}ions can be explained by several well-known mechanisms such as excited-state absorption (ESA) previously reported [32] as shown in **Figure. 11** and energy transfer up-conver-

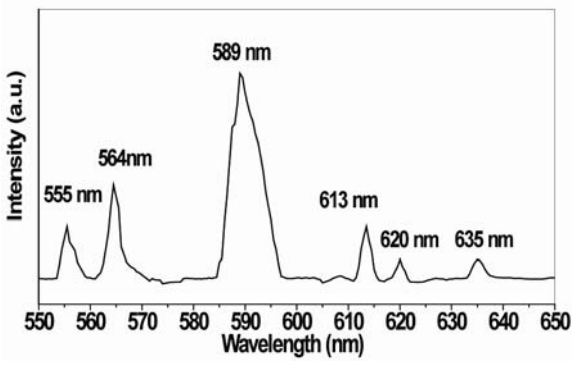

Figure 10 Room temperature Co-operative up-conversion emission spectra under laser diode excitation at 808 nm from monolithic [SiO_2:11P_2O_5:3Al_2O_3:1.2Er:1.8Yb], sintering at 300˚C.

sion (ETU). The ETU involves not only two closely neighboring Er^{3+} ions but also Er^{3+} and Yb^{3+} ions. When Yb^{3+} at $^4F_{5/2}$ state returns non-radiatively to the $^4F_{7/2}$ ground state, its energy is transferred to neighboring Er^{3+} in the $^4I_{11/2}$ state, and then this Er^{3+} ion was excited to the $^4F_{7/2}$ ($^2H_{11/2}$) state through the following channels: $^4I_{11/2}\rightarrow$ $^4F_{7/2}$ and $^4I_{13/2} \rightarrow {}^4F_{9/2}$. This is the main pathway by which Yb^{3+} sensitizes the up-conversion process.

After wards, excited Er^{3+} ions at $^4I_{13/2}$ level will take one ion to the $^4I_{9/2}$ level. This step followed by other successive transfer processes from ions at the $^4I_{13/2}$ state, which results in the excitation to higher levels. After non-radiative decay to lower states, radiative transitions to the ground state give rise to the observed red up-converted fluorescence [32].

4. Conclusions

Nano-composite silica-phosphate glasses activated by Er^{3+}: Yb^{3+} ions planar waveguides [SiO_2:11P_2O_5:3Al_2O_3: 1.2Er:(1.2, 1.8 and 3)Yb] were successfully prepared by sol–gel technique, in two forms monolithic and thin film by using spin-coating method. This as-synthesized sol was doped with 3 mol% Al^{3+} ions, to eliminate the OH groups and to increase the solubility of Re^{3+} ions. The structure of the prepared samples was evaluated by using XRD. One can conclude that the degree of crystallinity and the crystallite sizes of the trivalent Er^{3+} and Yb^{3+} ions dispersed in silica-phosphate host samples as thin film and monolith were increased by increasing both the concentrations of Er^{3+} and Yb^{3+} ions, and the increase in the sintering heat treatment temperature.

The values of the refractive index (n) of thin film samples are given at wavelength = 500 nm. It was found that it increase by increasing the sintering temperature and the

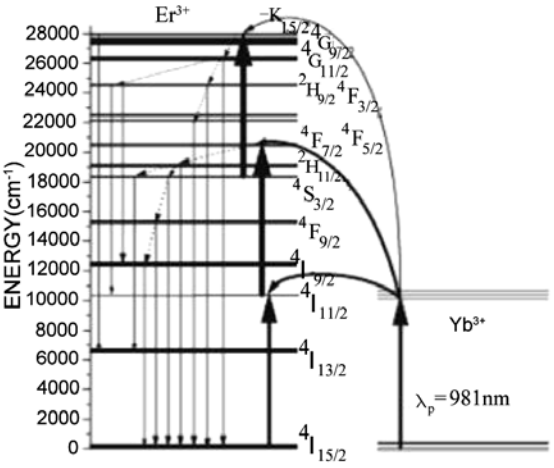

Figure 11. The energy level diagram of the green and red up-conversion emissions from the Er^{3+} and Yb^{3+} ions [32]

Yb^{3+} ions concentration from 1.55 up to 1.68. The obtained data allow the preparation of low loss coupling systems planar waveguide.

The visible and red Photoluminescence implies that the position of the emission peaks in the spectra corresponding to excitation by Argon laser light with wavelength 488 nm. It was due to transitions inside erbium ions corresponding to intra-4f transition of Er^{3+} and Yb^{3+} ions assigned to $^2H_{11/2}\rightarrow {}^4I_{15/2}$, $^4S_{3/2}\rightarrow$ $^4I_{15/2}$ and $^4F_{9/2}\rightarrow {}^4I_{15/2}$ for the monolith and thin film silica –phosphate planar wave guide. The red emissions in region between 600 - 700 nm are assigned to $^4F_{9/2}\rightarrow {}^4I_{15/2}$ transitions of Er^{3+} ions and its intensity increased with increasing the concentrations of Yb^{3+} ions in case of monolithic sample.

REFERENCES

[1] D. Barbier, "Integrated Optical Circuits and Components: Design and Applications," Dekker, New York, 1999.

[2] N. N. Khimich, G. M. Berdichevskii, E. N. Poddenezhnyi, V. V. Golubkov, A. A. Boiko, V. M. Ken'ko, O. B. Evreinov and L. A. Koptelova, "Sol-Gel Synthesis of an Optical Silica Glass Doped with Rare-Earth Elements," *Glass Physics and Chemistry*, Vol. 33, No. 2, 2007, pp. 152-155. doi:10.1134/S1087659607020095

[3] C. J. Brinker, A. J. Hurd, P. R. Schunk, G. C. Frye and C. S. Ashley, "Review of Sol Gel Thin Film Formation," *Journal of Non-Crystalline Solids*, Vol. 147-148, 1992, pp. 424-436. doi:10.1016/S0022-3093(05)80653-2

[4] B. E. Yoldas and I. K. Lloyd, "Nasicon Formation by Chemical Polymerization," *Materials Research Bulletin*, Vol. 18, No. 10, 1983, pp. 1171-1177. doi:10.1016/0025-5408(83)90019-3

[5] I. K. Battisha, M. A. Salem, A. M. S. El Nahrawy, Y. Badr, M. Kamal and B. Elouady, "Erbium Activated Monolith Silica-Phosphate Glasses Planar Waveguide and Up-Conversion Mechanism," *International Journal of Nano and Biomaterials*, Vol. 2, No. 1-5, 2009, pp. 191-203.

[6] A. J. Silversmith, N. T. T. Nguyen, B. W. Sullivan, D. M. Boye, C. Ortiz and K. R. Hoffman, "Rare-Earth Ion Distribution in Sol-Gel Glasses Co-doped with Al^{3+}," *Journal of Luminescence*, Vol. 128, No. 5-6, 2008, pp. 931-933. doi:10.1016/j.jlumin.2007.11.049

[7] Z. Xiao, B. Zhou, L. Yan, F. Zhu, F. Zhang and A. Huang, "Photoluminescence and Energy Transfer Processes in Rare Earth Ion Doped Oxide Thin Films with Substrate Heating," *Physics Letters A*, Vol. 374, No. 10, 2010, pp. 1297-1300. doi:10.1016/j.physleta.2010.01.017

[8] A. Martucci, A. Chiasera, M. Montagna and M. Ferrari, "Erbium-Doped GeO_2-TiO_2 Sol-Gel Waveguides," *Journal of Non-Crystalline Solids*, Vol. 322, No. 1-3, 2003, pp. 295-299. doi:10.1016/S0022-3093(03)00218-7

[9] B. Y. Ahn, S. I. Seok, S. Hong, J. S. Oh, H. Jung and W. J. Chung, "Optical Properties of Organic/Inorganic Nano-

composite Sol-Gel Films Containing $LaPO_4$: Er, Yb Nanocrystals," *Optical Materials*, Vol. 28, No. 4, 2006, pp. 374-379. doi:10.1016/j.optmat.2005.02.003

[10] R. Almeida, X. Min du, D. Barbier and X. Orignc, "Er^{3+}-Doped Multicomponent Silicate Glass Planar Waveguides Prepared by Sol-Gel Processing," *Journal of Sol-Gel Science and Technology*, Vol. 14, No. 2, 1999, pp. 209-216. doi:10.1023/A:1008794202103

[11] M. J. F. Digonnet, "Rare-Earth-Doped Fiber Lasers and Amplifiers," 2nd Edition, Dekker, New York, 2001. doi:10.1201/9780203904657

[12] M. J. F. Digonnet and E. Snitzer, "In Rare Earth Doped Fiber Lasers and Amplifiers," In: M. J. F. Digonnet, Ed., Marcel Dekker, New York, 1993, Chapter 5.

[13] Ph. Massiot, M. A. Centeno, I. Carrizosa and J. A. Odriozola, "Thermal Evaluation of Sol-Gel-Obtained Phosphosilicate Solids (Sipo)," *Journal of Non-Crystalline Solids*, Vol. 292, 2001, pp. 158-166. doi:10.1016/S0022-3093(01)00854-7

[14] T. L. Weeding, B. H. W. S. de Jong, W. S. Veeman and B. G. Aitken, "Silicon Coordination Changes from 4-Fold to 6-Fold on Devitrification of Silicon Phosphate Glass," *Nature*, Vol. 318, 1982, pp. 351-352. doi:10.1038/318352a0

[15] Ph. Massiot, M. A Centeno, M. Gouriou, M. I. Dominguez and J. A. Odriozola, "Sol-Gel Obtained Silicophosphates as Materials to Retain Caesium at High Temperatures," *Journal of Materials Chemistry*, Vol. 13, No. 1, 2003, pp. 67-74. doi:10.1039/b208698k

[16] S. P. Szu, L. C. Klein and M. Greenblatt, "Effect of Precursors on the Structure of Phosphosilicate Gels: ^{29}Si and ^{31}P MAS-NMR Study," *Journal of Non-Crystalline Solids*, Vol. 143, 1992, pp. 21-30. doi:10.1016/S0022-3093(05)80548-4

[17] D. Qiu, P. Guerry, J. C. Knowles, M. E. Smith and R. J. Newport, "Formation of Functional Phosphosilicate Gels from Phytic Acid and Tetraethyl Orthosilicate," *Journal of Sol-Gel Science and Technology*, Vol. 48, No. 3, 2008, pp. 378-383. doi:10.1007/s10971-008-1818-9

[18] R. P. Rao and D. J. Devine, "RE-Activated Lanthanide Phosphate Phosphors for PDP Applications," *Journal of Luminescence*, Vol. 87-89, 2000, pp. 1260-1263. doi:10.1016/S0022-2313(99)00551-7

[19] J. Dhanaraj, M. Geethalakshmi, R. Jagannathan and T. R. N. Kutty, "Eu^{3+}-Doped Yttrium Oxysulfide Nanocrystals—Crystallite Size and Luminescence Transition(s)," *Journal of Chemical Physics Letters*, Vol. 387, No. 1-3, 2004, pp. 23-28. doi:10.1016/j.cplett.2004.01.079

[20] J. A. Sampaio, M. L. Baesso, S. Gama, A. A. Coelho, J. A. Eiras and I. A. Santos, "Rare Earth Doping Effect on the Elastic Moduli of Low Calcium Aluminosilicate Glasses," *Journal of Non-Crystalline Solids*, Vol. 304, No. 1-4, 2002, pp. 293-298. doi:10.1016/S0022-3093(02)01037-2

[21] M. T. Wang and J. S. Cheng, "Viscosity and Thermal Expansion of Rare Earth Containing Soda-Lime-Silicate Glass," *Journal of Alloys and Compounds*, Vol. 504, No. 1, 2010, pp. 273-276. doi:10.1016/j.jallcom.2010.08.134

[22] N. Kitamura, K. Fukumi, J. Nishii and N. Ohno, "Relationship between Refractive Index and Density of Synthetic Silica Glasses," *Journal of Non-Crystalline Solids*, Vol. 101, No. 12, 2009, pp. 123533-123540.

[23] S. Shen, W. H. Chow, D. P. Steenson and A. Jha, "Fabrication of Er^{3+}-Doped Oxyfluoride-Silicate Glass Film by Pulsed Laser Deposition for Planar Amplifier," *Journal of Non-Crystalline Solids*, Vol. 355, No. 37-42, 2009, pp. 1893-1896.

[24] E. T. Y. Lee and E. R. M. Taylor, "Compositional Effects on the Optical and Thermal Properties of Potassium Aluminophosphate Glasses," *Optical Materials*, Vol. 27, No. 2, 2004, pp. 323-330. doi:10.1016/j.optmat.2004.02.029

[25] S. N. Houde-Walter, P. M. Peters, J. F. Stebbins and Q. Zeng, "Hydroxyl-Contents and Hydroxyl-Related Concentration Quenching in Erbium Doped Aluminophosphate, Aluminosilicate and Fluorosilicate Glasses," *Journal of Non-Crystalline Solids*, Vol. 286, No. 1-2, 2001, pp. 118-131. doi:10.1016/S0022-3093(00)00445-2

[26] P. Yang, M. K. Lu, C. F. Song, D. Xu, D. R. Yuan and F. Gu, "Photoluminescence Properties of Alkaline Metallic Ions Doped Sol-Gel Silica Glasses," *Materials Science & Engineering*, Vol. B90, No. 1-2, 2002, pp. 99-102. doi:10.1016/S0921-5107(01)00929-1

[27] V. Y. Timoshenko, D. M. Zhigunov, P. K. Kashkarov, O. A. Shalygina, S. A. Teterukov, R. J. Zhang, M. Zacharias, M. Fujii and Sh. Hayashi, "Photoluminescence Properties of Erbium-Doped Structures of Silicon Nanocrystals in Silicon Dioxide Matrix," *Journal of Non- Crystalline Solids*, Vol. 352, No. 9-20, 2006, pp. 1192- 1195.

[28] V. V. Filippov, P. P. Pershukevich, V. V. Kuznetsova and V. S. Homenko, "Photoluminescence Excitation Properties of Porous Silicon with and without Er^{3+}-Yb^{3+}-Containing Complex," *Journal of Luminescence*, Vol. 99, No. 3, 2002, pp. 185-195.

[29] C. Li, B. Dong, S. Li and C. Song, "Er^{3+}-Yb^{3+} Co-Doped Silicate Glass for Optical Temperature Sensor," *Chemical Physics Letters*, Vol. 443, No. 4-6, 2007, pp. 426-429.

[30] R. M. Almeida, A. C. Marques and S. Portal, "Glassy and Nano-Crystalline Photonic Materials and Structures by Sol-Gel," *Optical Materials*, Vol. 27, No. 11, 2005, pp. 1718-1725.

[31] J. Z. Wang, Z. Q. Shi, Y. Shi, L. Pu, L. J. Pan, R. Zhang, Y. D. Zheng, Z. S. Tao and F. Lu, "Broad Excitation of Er Luminescence in Er-Doped HfO_2 Films," *Applied Physics A*, Vol. 94, No. 2, 2009, pp. 399-403.

[32] B. Dong, C. R. Li and M. K. Lei, "Green and Red Up-Conversion Emissions of Er^{3+}-Yb^{3+} Codoped Al_2O_3 Powders Prepared by the Nonaqueous Sol-Gel Method," *Journal of Luminescence*, Vol. 126, No. 2, 2007, pp. 441-446.

